AFRL-RQ-WP-TP-2018-0015

PRESSURE SCALINGS AND INFLUENCE REGION RESEARCH

James H. Miller

High Speed Systems Division

JANUARY 2018

AIR FORCE RESEARCH LABORATORY
AEROSPACE SYSTEMS DIRECTORATE
WRIGHT-PATTERSON AIR FORCE BASE, OH 45433-7542
AIR FORCE MATERIEL COMMAND
UNITED STATES AIR FORCE

NOTICE AND SIGNATURE PAGE

Using Government drawings, specifications, or other data included in this document for any purpose other than Government procurement does not in any way obligate the U.S. Government. The fact that the Government formulated or supplied the drawings, specifications, or other data does not license the holder or any other person or corporation; or convey any rights or permission to manufacture, use, or sell any patented invention that may relate to them.

This report was cleared for public release by the USAF 88th Air Base Wing (88 ABW) Public Affairs Office (PAO) and is available to the general public, including foreign nationals.

Copies may be obtained from the Defense Technical Information Center (DTIC) (http://www.dtic.mil).

AFRL-RQ-WP-TP-2018-0015 HAS BEEN REVIEWED AND IS APPROVED FOR PUBLICATION IN ACCORDANCE WITH ASSIGNED DISTRIBUTION STATEMENT.

*//Signature//
JAMES H. MILLER
Project Manager/Principal Advisor
High Speed Systems Division
Aerospace Systems Directorate

//Signature//
JOHN G. DAYTON, Chief
Vehicle Technology Branch
High Speed Systems Division
Aerospace Systems Directorate

//Signature//
ROBERT A. MERCIER
Deputy for Technology
High Speed Systems Division
Aerospace Systems Directorate

This report is published in the interest of scientific and technical information exchange, and its publication does not constitute the Government's approval or disapproval of its ideas or findings.

*Disseminated copies will show "//Signature//" stamped or typed above the signature blocks.

REPORT DOCUMENTATION PAGE

Form Approved
OMB No. 0704-0188

1. REPORT DATE *(DD-MM-YY)*	2. REPORT TYPE	3. DATES COVERED *(From - To)*
January 2018	Technical Paper	01 July 2015 – 01 January 2018

4. TITLE AND SUBTITLE
PRESSURE SCALINGS AND INFLUENCE REGION RESEARCH

5a. CONTRACT NUMBER
In-house

5b. GRANT NUMBER

5c. PROGRAM ELEMENT NUMBER
62201F

6. AUTHOR(S)
James H. Miller

5d. PROJECT NUMBER
2405

5e. TASK NUMBER
N/A

5f. WORK UNIT NUMBER
Q1K7

7. PERFORMING ORGANIZATION NAME(S) AND ADDRESS(ES)
High Speed Systems Division (AFRL/RQH)
Air Force Research Laboratory, Aerospace Systems Directorate
Wright-Patterson Air Force Base, OH 45433-7542
Air Force Materiel Command, United States Air Force

8. PERFORMING ORGANIZATION REPORT NUMBER
AFRL-RQ-WP-TP-2018-0015

9. SPONSORING/MONITORING AGENCY NAME(S) AND ADDRESS(ES)
Air Force Research Laboratory
Aerospace Systems Directorate
Wright-Patterson Air Force Base, OH 45433-7542
Air Force Materiel Command
United States Air Force

10. SPONSORING/MONITORING AGENCY ACRONYM(S)
AFRL/RQH

11. SPONSORING/MONITORING AGENCY REPORT NUMBER(S)
AFRL-RQ-WP-TP-2018-0015

12. DISTRIBUTION/AVAILABILITY STATEMENT
DISTRIBUTION STATEMENT A: Approved for public release. Distribution is unlimited.

13. SUPPLEMENTARY NOTES
PA Case Number: 88ABW-2018-0341; Clearance Date: 26 Jan 2018.

14. ABSTRACT

An updated non-dimensional approach for pressure is used to normalize the Navier-Stokes equations and the results are briefly discussed. Additionally, updated experimental results are presented along with discussion of collaborative research efforts in asymptotic theory and application of computational fluid dynamics (CFD) methods to utilize influence regions to improve computational efficiency when changes in geometry become a significant driver to computational analysis timelines.

15. SUBJECT TERMS
supersonic, shock-boundary layer interaction, upstream influence, influence regions, similarity parameters

16. SECURITY CLASSIFICATION OF:			17. LIMITATION OF ABSTRACT:	18. NUMBER OF PAGES	19a. NAME OF RESPONSIBLE PERSON (Monitor)
a. REPORT	b. ABSTRACT	c. THIS PAGE			James H. Miller
Unclassified	Unclassified	Unclassified	SAR	14	19b. TELEPHONE NUMBER *(Include Area Code)* N/A

Pressure Scalings and Influence Region Research

James H. Miller[1]

Air Force Research Laboratory, Wright-Patterson AFB 45433

Nomenclature

C_p = pressure coefficient, $C_p = \frac{p-p_\infty}{{}^1/_2\,\rho_\infty V_\infty^2}$

l = length of elliptic region, *m*

L = reference length, *m*

$\frac{l_u}{\delta_L}$ = ratio of upstream influence length to undisturbed (flat plate) boundary layer thickness

$\frac{l}{\delta_L}$ = ratio of elliptic region length to undisturbed (flat plate) boundary layer thickness

l_u = upstream influence length, *m*

l_d = downstream influence length, *m*

M = Mach number, ratio of velocity to speed of sound, $M = \frac{V}{\sqrt{\gamma\,p/\rho}}$

p = pressure, N/m^2

Re = Reynolds number, ratio of inertia forces to viscous forces, $Re = \frac{\rho_\infty V_\infty L}{\mu_\infty}$

t = time, *s*

u,v,w = Cartesian velocity components in the *x,y,z* directions respectively, *m/s*

V_∞ = reference or freestream velocity, *m/s*

x,y,z = Cartesian coordinates, *m*

Δp = reference change in pressure (assumed positive) relative to freestream (e.g., $p_c - p_\infty$, where p_c is the inviscid pressure downstream of a shock interaction with a flat surface or compression ramp), N/m^2

δ_L = boundary layer thickness at location *L, m*

γ = ratio of specific heats, 1.4 for air.

θ = compression ramp angle, degrees

[1] Principal Advisor, High Speed Systems Division, AFRL/RQH, B18A, Rm A005, 1950 5th Street, Wright-Patterson AFB OH, 45433.

τ = shear stress, N/m^2

μ = viscosity, $kg / (m\ s)$

Superscripts:

~ = nondimensional quantity normalized by freestream conditions or reference change in pressure

Subscripts:

d = downstream boundary of elliptic region

L = *x* location of compression ramp leading edge or shock impingement point

Δ = Reference change in pressure (usually post-shock pressure – freestream pressure)

u = upstream boundary of elliptic region

xx,xy = Cartesian components of shear stress

∞ = freestream conditions

I. Introduction

In a recent technical note [1], there was an assertion that a new similarity variable was developed for the Navier-Stokes equations. This new variable was used to define correlation functions for supersonic flows with upstream and downstream influence, where the influence lengths are defined in terms of a-priori quantities (freestream conditions and undisturbed boundary layer thicknesses) for adiabatic walls. In the present work, an updated non-dimensional approach for pressure is used to normalize the governing equations and the result is briefly discussed. Additionally, updated experimental results are presented along with discussion of collaborative research efforts in asymptotic theory and application of CFD methods to utilize influence regions to improve computational efficiency when changes in geometry become a significant driver to computational analysis timelines.

II. Alternate Pressure Scaling

In the present discussion we focus on the 2D compressible momentum equation in the Cartesian x direction [2]:

$$\frac{\partial \rho u}{\partial t} + \frac{\partial}{\partial x}[\rho u^2 + p - \tau_{xx}] + \frac{\partial}{\partial y}[\rho uv - \tau_{xy}] = 0$$

with

$$\tau_{xx} = \frac{2}{3}\mu\left(2\frac{\partial u}{\partial x} - \frac{\partial v}{\partial y}\right);\ \tau_{xy} = \mu\left(\frac{\partial u}{\partial y} + \frac{\partial v}{\partial x}\right)$$

In the following nondimensionalization approach, nondimensional quantities are annotated with a tilde:

$$\tilde{x},\tilde{y} = \frac{x}{L},\frac{y}{L};\ \tilde{t} = \frac{t}{L/V_\infty};\ \tilde{\rho} = \frac{\rho}{\rho_\infty};\ \tilde{u},\tilde{v} = \frac{u}{V_\infty},\frac{v}{V_\infty};\ \tilde{p} = \frac{p}{\mu_\infty\frac{V_\infty}{L}};\ \tilde{\mu} = \frac{\mu}{\mu_\infty}$$

As in the previous work, the pressure is nondimensionalized differently than traditional methods, but in the present case, the pressure is nondimensionalized by a representative shear force defined by freestream conditions. This could be viewed as the ratio of pressure forces to shear forces. Substituting for the dimensional quantities in the momentum equation, and then rearranging terms and simplifying leads to the following equation in nondimensional form:

$$\frac{\partial\tilde{\rho}\tilde{u}}{\partial\tilde{t}} + \frac{\partial}{\partial\tilde{x}}[\tilde{\rho}\tilde{u}^2 + \frac{1}{Re}[\,\tilde{p} - \tilde{\tau}_{xx}\,]] + \frac{\partial}{\partial\tilde{y}}\left[\tilde{\rho}\tilde{u}\tilde{v} - \frac{1}{Re}\tilde{\tau}_{xy}\right] = 0$$

It's useful to recognize that the product $\frac{\check{p}}{Re}$ is equal to the conventional approach to non-dimensionalizing pressure, namely, $\frac{\check{p}}{Re} = \frac{p}{\rho_\infty V_\infty^2}$, which is independent of Reynolds number. It is also important to note that as Reynolds number becomes large due to reduced viscosity, $\check{p}$ also becomes large. Also, it now becomes more straightforward to compare pressure forces to shear forces since they would be nondimensionalized using the same approach. These types of comparisons may be discussed in future work.

The impact of choosing the above nondimensionalization can be better seen after imposing assumptions as is traditionally done in boundary layer theory [3]. Let the streamwise shear stress be much smaller than the pressure; the normal velocity gradient with respect to x is much smaller than the axial velocity gradient with respect to y; and the viscous layer is confined to a small distance from the body (δ). Mathematically, this can be represented by:

$$\tilde{p} \gg \tilde{\tau}_{xx};\quad \frac{\partial\tilde{u}}{\partial\tilde{y}} \gg \frac{\partial\tilde{v}}{\partial\tilde{x}};\quad L \gg \delta$$

assuming steady flow, the x-momentum equation becomes:

$$\frac{\partial}{\partial\tilde{x}}[\tilde{\rho}\tilde{u}^2 + \frac{1}{Re}\,\tilde{p}\,] + \frac{\partial}{\partial\tilde{y}}\left[\tilde{\rho}\tilde{u}\tilde{v} - \frac{1}{Re}\,\tilde{\mu}\frac{\partial\tilde{u}}{\partial\tilde{y}}\right] = 0$$

or

$$\frac{\partial}{\partial \tilde{x}}[\tilde{\rho}\tilde{u}^2] + \frac{\partial}{\partial \tilde{y}}[\tilde{\rho}\tilde{u}\tilde{v}] + \frac{1}{Re}\left[\frac{\partial \tilde{p}}{\partial \tilde{x}} - \frac{\partial}{\partial \tilde{y}}\tilde{\mu}\frac{\partial \tilde{u}}{\partial \tilde{y}}\right] = 0$$

and taking the Reynolds number terms to the right hand side:

$$\frac{\partial}{\partial \tilde{x}}[\tilde{\rho}\tilde{u}^2] + \frac{\partial}{\partial \tilde{y}}[\tilde{\rho}\tilde{u}\tilde{v}] = \frac{1}{Re}\left[\frac{\partial}{\partial \tilde{y}}\tilde{\mu}\frac{\partial \tilde{u}}{\partial \tilde{y}} - \frac{\partial \tilde{p}}{\partial \tilde{x}}\right]$$

Now it is hopefully clear from the above equation that the difference between the nondimensional shear stress and streamwise pressure gradient must be of the order of Re to keep the equation balanced, or:

$$Re \sim \left(\frac{\partial}{\partial \tilde{y}}\tilde{\mu}\frac{\partial \tilde{u}}{\partial \tilde{y}} - \frac{\partial \tilde{p}}{\partial \tilde{x}}\right)$$

and

$$Re \sim \left(\frac{1}{\frac{\delta}{L}}\tilde{\mu}\frac{1}{\frac{\delta}{L}} - \frac{\partial \tilde{p}}{\partial \tilde{x}}\right)$$

If the nondimensional viscosity has order 1 magnitude (which may be an oversimplification, but for argument sake we adopt it here), then the result is that

$$Re \sim \left(\frac{1}{\frac{\delta}{L}}\frac{1}{\frac{\delta}{L}} - \frac{\partial \tilde{p}}{\partial \tilde{x}}\right)$$

solving for the boundary layer thickness yields:

$$\frac{\delta}{L} \sim \frac{1}{\sqrt{\left(Re - \frac{\partial \tilde{p}}{\partial \tilde{x}}\right)}}$$

Or in words, the nondimensional boundary layer thickness is inversely proportional to the square root of the difference between the Reynolds number and the nondimensional streamwise pressure gradient. This differs from conventional boundary layer theory results but appear to be consistent. The present result implies a growth of the boundary layer

for adverse pressure gradients and a reduction of the boundary layer thickness for favorable pressure gradients. Further investigation into the implications of these results may be addressed in future work.

III. Compression Ramp Correlations as Functions of Interaction Parameter

Previously in [1], correlations of upstream and downstream influence were shown for laminar compressive flows (compression ramps and shock impingements) in terms of the similarity parameter $\frac{Re\ Cp}{2}$, or interaction parameter. In the present work, we show the results obtained for upstream influence of compression ramps for both laminar and turbulent flows in Fig. 1.

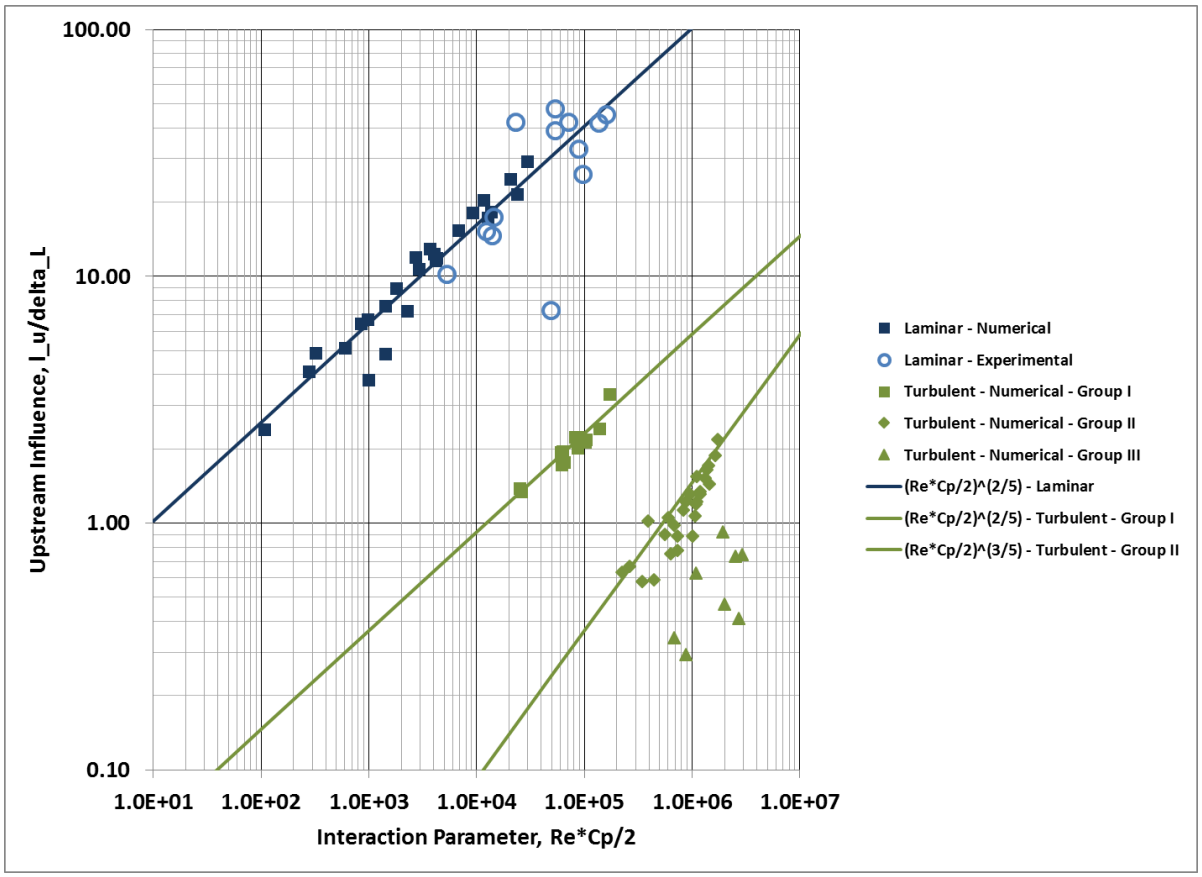

Figure 1: Correlation Results for Upstream Influence to 2D Compression Ramps and Shock Impingement Flowfields

In this figure, it is clear that the interaction parameter generally increases with upstream influence, but the slope of the upstream influence appears to be a function of Reynolds number for turbulent flows, while for laminar flows the

upstream influence varies as the interaction parameter raised to the 2/5 power. This result is similar in character to that of incompressible pipe flow and the Moody diagram [4] where the friction factor varies at constant slope with Reynolds number independent of pipe roughness, while for turbulent flow, the slope does depend on pipe roughness. The experimental and numerical data for laminar adiabatic wall conditions was taken for ramps [5] from previous work. The numerical data for turbulent flow was taken from the work of Ramesh et al. [6].

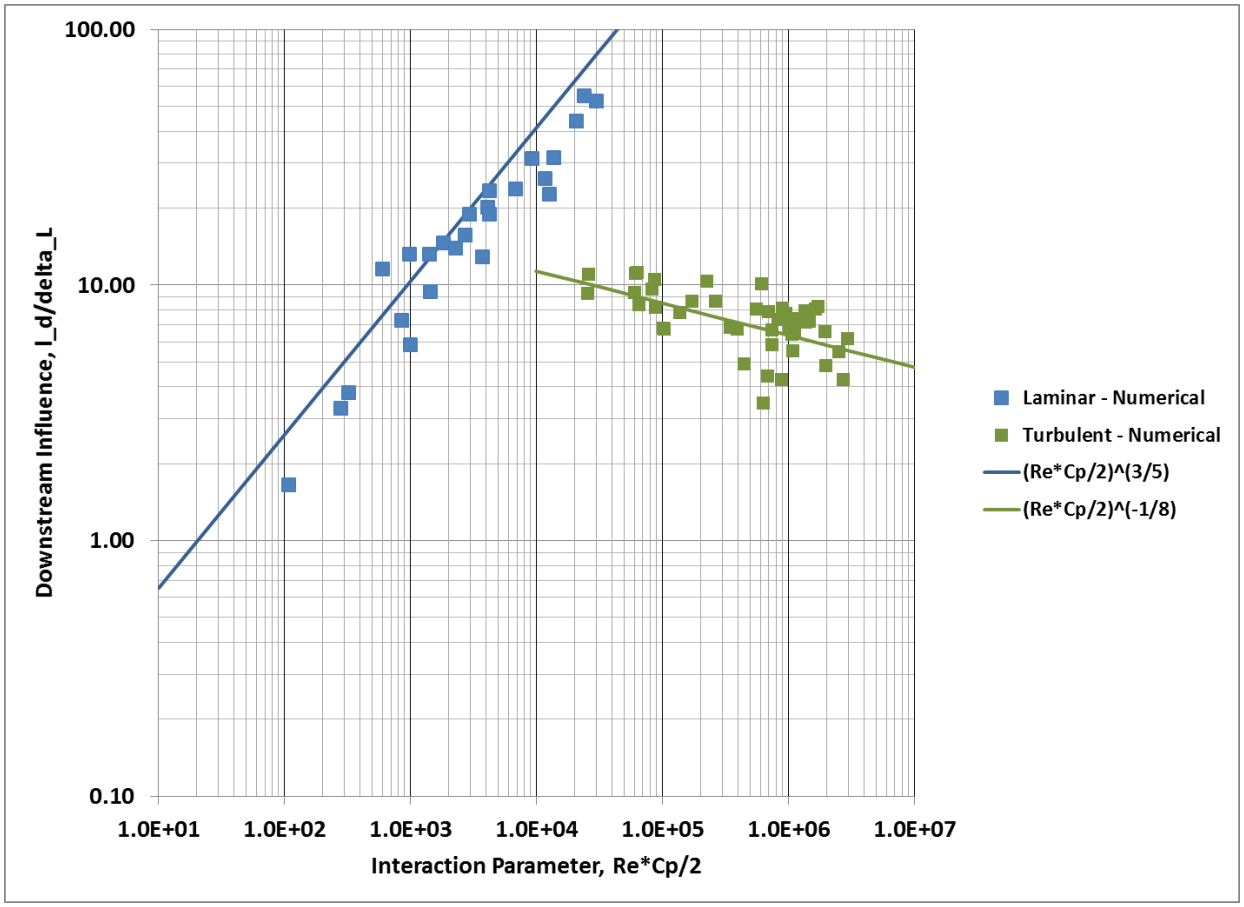

Figure 2: Results for downstream influence length vs. Interaction Parameter

Figure 2 has the results for the downstream influence length vs. the interaction parameter in both laminar and turbulent flows. These numerical results indicate that the downstream influence length increases with increasing interaction parameter for laminar flows, while it slightly decreases for turbulent flows (with larger scatter).

IV. Experimental Results

From Oct. 2015 to Feb. 2016, testing was performed on the copper flat plate model of the Mach 6 Influence Boundaries program. This testing was completed in the Mach 6 High Reynolds Number Facility at Wright-Patterson AFB [7]. The model was a flat plate and an earlier version of the CAD geometry is shown in Figure 3.

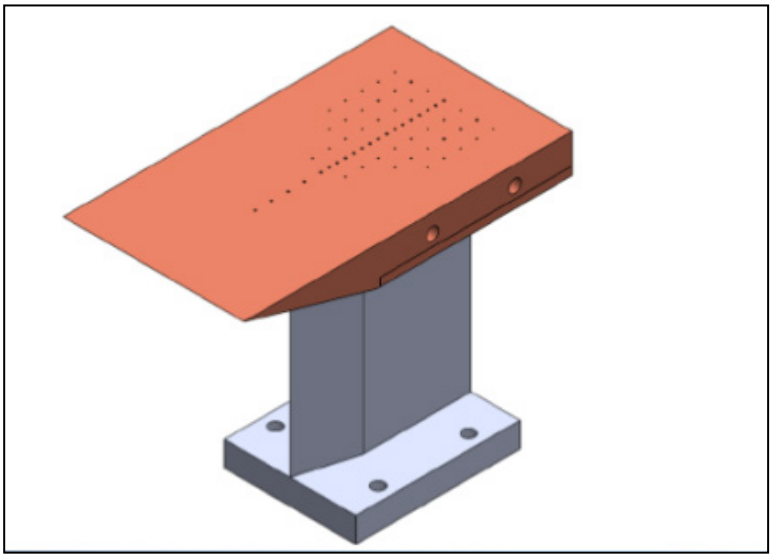

Figure 3 Flat Plate model geometry with support strut.

Over 60 runs were completed with the flat plate model. Conditions and results will be documented in a future report. A key capability for this program was to establish the capability to determine the boundary layer thickness near the X=7" station, where the models to be used in future tests will have a compression ramp juncture. Sample results are shown in Figure 4. On the graph in the upper left there are peak intensities showing the growth of the boundary layer as the axial station increases. In addition, the two graphs in the lower right show numerical predictions of the boundary layer thickness for the X=7" station. The approximate height from these results is about 0.1' which is consistent with the measured experimental results.

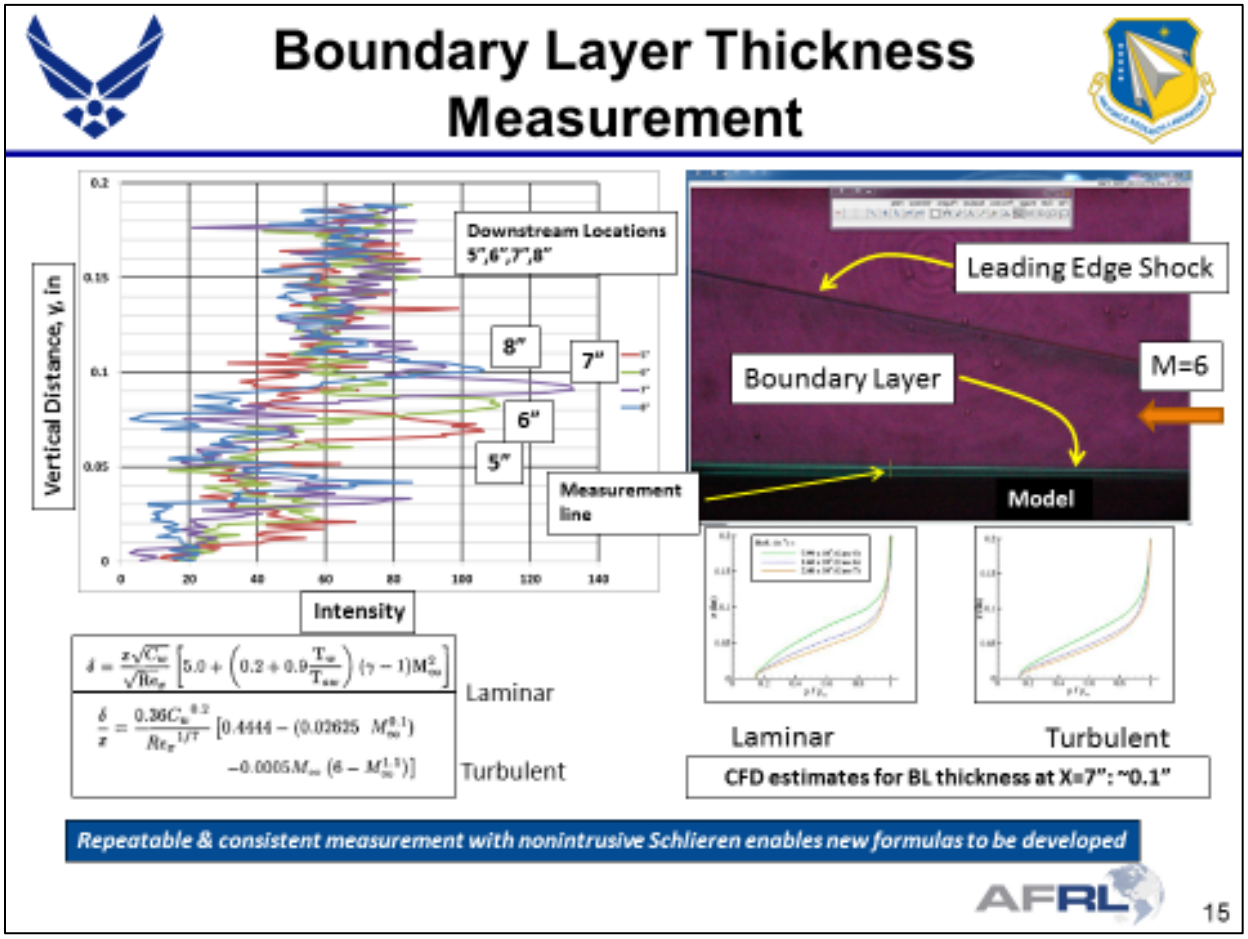

Figure 4 Sample results with boundary layer measurements.

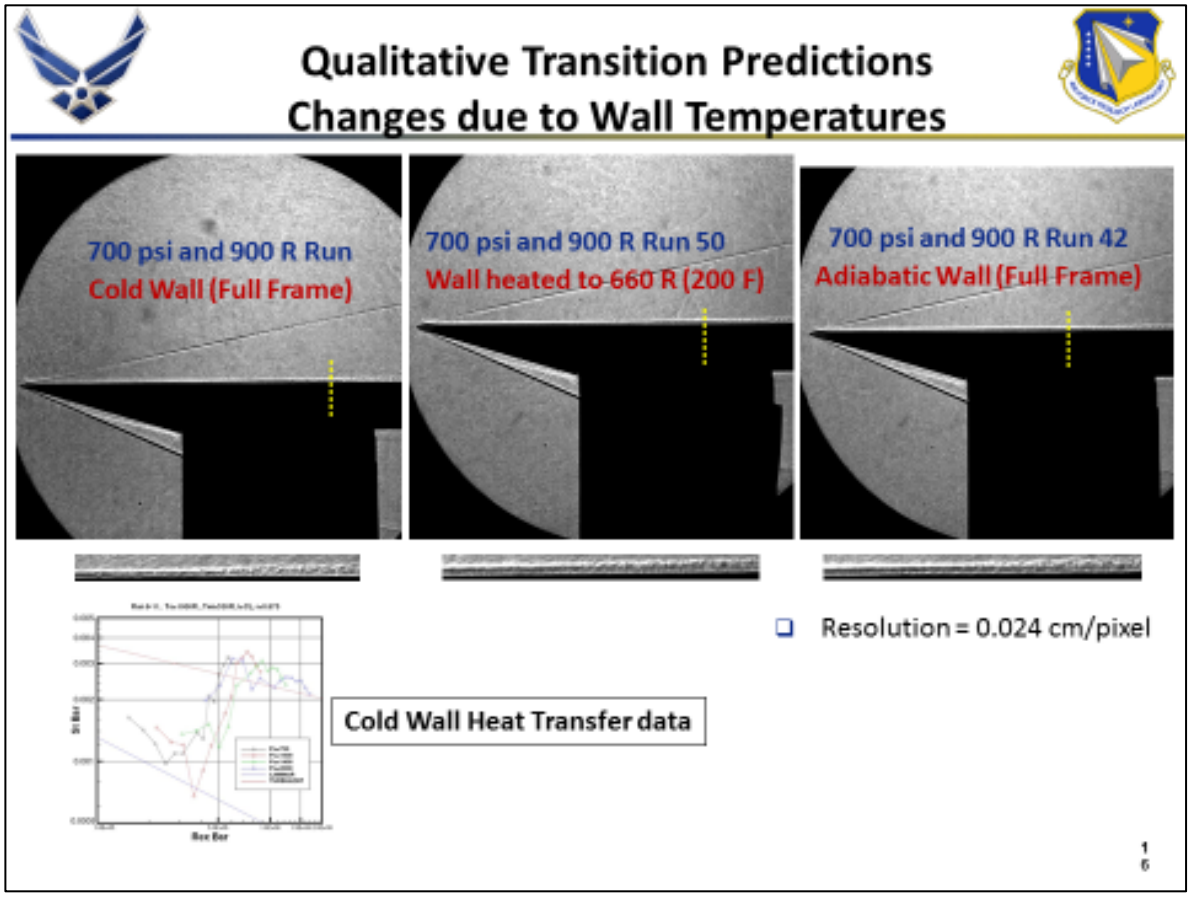

Figure 5 Sample Schlieren results with effects from wall temperatures.

In Figure 5, preliminary results show the approximate boundary layer transition location based on the observation of acoustic wave structures in the boundary layer corresponding to the onset of turbulence [8]. An important goal of the testing was to establish data at conditions for an adiabatic wall so that previous data could be used in verifying correlations [5,6]. Adiabatic conditions were achieved through pre-heating of the model before starting the tunnel. More details on this approach will be discussed in a future report.

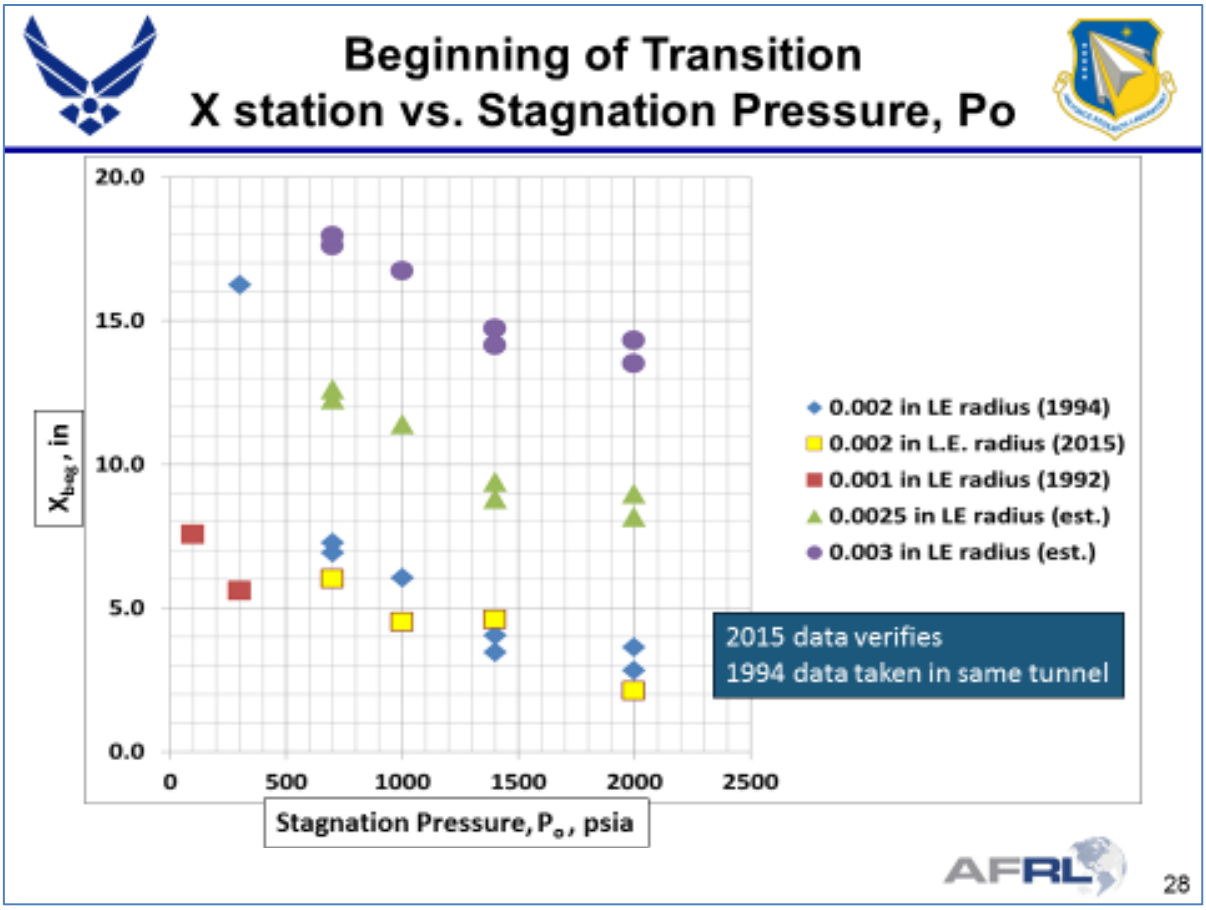

Figure 6 Beginning of transition location as a function of stagnation pressure and leading edge radius.

In Figure 6, preliminary results show the approximate boundary layer transition location based on the measured heat transfer for cold wall conditions. Attempts were made to match the conditions used by Frew et al. [7] in the same tunnel over 20 years prior to the present testing. The present results are in good overall agreement with the past results. In addition, it is important to note that the leading edge radius of the plate affects the transition location with a larger radius producing a more laminar flowfield.

V. Collaborative Research Activities

At the time of this writing, two collaborative research efforts have begun. At Iowa State University, an asymptotic theoretical approach is to be applied to high Reynolds number shock layer analysis to a compression ramp. Direct comparisons of the asymptotic theory to CFD calculations and scaling parameters described in Ref. 1 are also planned.

At the Air Force Academy, the premise of reducing computational times by a CFD building block approach is being explored for hypersonic configurations. More details on those two efforts will be presented in later reports.

VI. Conclusions

A new nondimensional approach for the pressure in the Navier-Stokes equations has been developed. This approach allows the boundary layer thickness to be written as a function of Reynolds number and streamwise pressure gradient. Both numerical and experimental data have been re-formulated in terms of the interaction parameter for compression ramp flows under laminar and turbulent conditions with adiabatic walls. A distinctive change in the upstream influence slope magnitude occurs when transitioning from laminar to turbulent. For the downstream influence, the slope changes magnitude and sign when transitioning from laminar to turbulent. The preliminary experimental results for a flat plate in a Mach 6 flowfield were also discussed. Boundary layer thicknesses were determined and laminar-turbulent transition was found to be consistent with previous results taken in the same tunnel two decades prior to the present test.

IV. References

[1] Miller, J.H., "Elliptic Length Scales in Laminar, Two-Dimensional Supersonic Flows," AFRL-RQ-WP-TP-2015-0109, June 2015.

[2] Tannehill, J.C., Anderson, D.A., and Pletcher, R.H., Computational Fluid Mechanics and Heat Transfer, 2nd ed., Taylor and Francis, Washington, DC, 1997, pp. 263-264.

[3] Schlichting, H., "Boundary Layer Theory," McGraw-Hill Book Company, 1979, pp. 127-131.

[4] Incropera, F.P., DeWitt, D.P., "Fundamentals of Heat and Mass Transfer," John Wiley & Sons, Inc., 1990, pp. 472-474.

[5] Miller, J.H., Tannehill, J.C., and Lawrence, S.L., "Parabolized Navier-Stokes Algorithm for Solving Supersonic Flows with Upstream Influences," *AIAA Journal*, Vol. 38, No. 10, Oct. 2000, pp. 1837-1845.

[6] Ramesh, M.D., and Tannehill, J.C., "Correlations to Predict the Streamwise Influence Regions in Supersonic Turbulent Flows," Journal of Aircraft, Vol. 41, No. 2, March-April 2004, pp. 274-283.

[7] Frew, D., Galassi, L. Stava, D., Azevedo, D. "A Study of Incipient Separation Limits for Shock-Induced Boundary Layer Separation for Mach 6 High Reynolds Flow," AIAA 93-2481, June 1993.

[8] Schneider, S.P., "Development of Hypersonic Quiet Tunnels," *Journal of Spacecraft and Rockets*, Vol. 45, No. 4, July-August 2008, pp. 641-664.